REMARKS

The present amendment is submitted in an earnest effort to advance this case to issue without delay.

1. The priority claim acknowledgement in paragraph 13 of PTO-326 is appreciated.

2. Pursuant to the Examiner's suggestion, a new title directed to the method and detailing the invention is provided herewith.

3. The new abstract required by the Examiner and directed to the method has been supplied.

4. Claims 1 and 19 have been amended to clarify the fact that the high energy beam is an electron beam and claim 6 has been cancelled as superfluous.

Claim 7 has been made directly dependent upon claim 1.

5. Claims 1 to 7 and 19 have been rejected under 35 USC 112, second paragraph as allegedly indefinite for failing to particularly point out and distinctly claim the subject matter which Applicant regards as the invention.

The terms "high" and "low" have been challenged by the

perfectly definite when the term is meaningful to persons skilled

in the art, say Ex parte Miller, 18 USPQ 216; Ex parte Brownell, 33 USPQ 242; and Ex parte Glover et al, 42 USPQ 636 and the host of cases following these which essentially say the same thing.

There are enclosed a number of publications derived from the internet and which support this position. For example, an enclosure A attached hereto is entitled, "Dynamics of surface chemical reactions induced by low-energy electrons: oxidation of hydrogen passivated Si by H_20". This article clearly demonstrates that "low energy electrons" is a term of art.

Enclosure B is entitled "Uniformity of High-Energy Electron-Beam Calibrations" demonstrating that "high energy electron beam" is a term of art.

Enclosure C is entitled "High-pressure nanolithography using low-energy electrons from a scanning tunnelling microscope".

Enclosure D is entitled "Energy deposition by low energy electrons in Ar and other gases".

Enclosure E is entitled "Stochastic Acceleration of Low Energy Electrons in Plasma with Finite Temperature".

Enclosure F is entitled "Holography with Low Energy Electrons: Principles and Applications".

From the foregoing, it will be apparent that the rejection under 35 USC 112, second paragraph based upon the user of the terms "high" and "low" is misplaced and should be withdrawn.

With respect to the objection to claim 1, line 22 under

6. The rejection of the claims as amended on Morton cannot stand.

The Morton reference has been applied to show that indeed everything in the admitted prior art of FIG. 1 is known and that is all that Morton discloses. The Examiner recognizes that Morton does not have a self bias and critical to the invention is the provision of a radio frequency or pulsed direct current plasma ahead of the substrate so that the surface of the substrate is bombarded with particles from the radio frequency or pulsed direct current plasma. The Examiner has referred to the radio frequency field at the substrate surface and more precisely Morton states at column 2, lines 38 to 60: "Briefly stated the optical thin film deposition system of the present invention comprises a vacuum chamber, substrate support and movement means for improving deposition uniformity, thermal and electron beam means for vaporizing solid materials, substrate heating means, inlet and outlet baffles for providing a laminar gas flow across the surface of substrates, and an antenna for providing an RF field at the substrate surface. The evaporative sources are used to deposit thin films of the solid materials being vaporized or to provide gases for reaction with other gases in a RPD or CVD process. The baffles are used to provide a flow of reactive gases across the substrate surface for RPD and CVD processes, but do not interfere with evaporative deposition. The RF antenna is used to generate a

provide optimum substrate temperatures for evaporative deposition

and RPD. Reactive plasma cleaning is used prior to any sequence of depositions and depositions are performed in any sequence without breaking vacuum or removing substrates from the chamber."

There is no teaching here of the radio frequency or pulsed direct current plasma with the effect of bombardment of the substrate.

That eliminates any residue optical absorption to allow the density of the deposited layer to be increased over the prior art.

The Morton reference, therefore, does not teach or suggest the claimed invention.

Applicant believes that the following statement may be helpful:

"Maybe it is useful to remember that the family of Ion Plating processes (invented by Mattox in the 1964) is generally constituted by a configuration in which is created a plasma in front of the substrates that energize a percentage of condensing particles (by ionizing it and than accelerated by the substrate bias) and/or by bombarding the growing film with ionized particles.

The USA patent 4,619,748 (of the firm Balzers) was an evolution of the previous Ion Plating configuration, in which the ionization of condensing particles is obtained by bombarding the evaporating material (heated by an electron gun) with a beam of low energy (around 60-80 eV) and by using the self-bias of the

Our invention is a further improvement of this patent based on the introduction of a R.F. (or D.C. pulsed) plasma in front of the substrates, with the scope to eliminate the residual optical absorption (always present by using previous configuration), to increase the density of the deposited layer and also to make possible an higher deposition rate, by enhancing the reactivity of the process atmosphere.

In more details as far as regarding the U.S. patent 4,058,638, this patent describes a conventional Ion Plating plasma assisted process, using traditional thermal source (emitting non ionized particles) and generic CVD system. In the process proposed by our invention the most important effects induced by the plasma surrounding the substrates are to enhance the reactivity of the process atmosphere to obtain absorption free optical coatings (by recovering the dissociation induced by the energetic bombardment up to 60-80 eV), to energize the condensing ionized particles and to introduce a controlled ion bombardment of the growing film. Regarding the United States Patent 6,315,873, this patent describes a traditional Reactive Sputtering configuration with the introduction of fluorinate gases near to the substrates to deposit fluorite materials starting from metal. In this case this technique is not even an Ion Plating process and than very different from our invention.

Regarding the USA patent 6,045,671 this is just a masking

Finally regarding the USA patent 6,081,287 this describes a thermal head and I don't see any contact with our invention."

Since the claims in the case are deemed to be allowable, an early notice to that effect is earnestly solicited.

7. A petition for an automatic one month extension of the term is enclosed together with a PTO-2038 form charging the amount to a credit card of the undersigned.

Respectfully submitted,
The Firm of Karl F. Ross P.C.

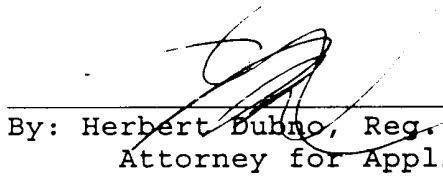

By: Herbert Dubno, Reg. No. 19,752
Attorney for Applicant

DB-
DATED: 3 October 2003

5676 Riverdale Avenue Box 900
Bronx, NY 10471-0900
Cust. No.: 535
Tel: (718) 884-6600
Fax: (718) 601-1099

Encls: Copies of Publications
Petition for Extension
PTO-2308 Form

(A)

▪ Previous abstract ▪ Next abstract

Session H33 - Postdeadline Poster Session II
POSTER session, Tuesday evening, March 19
Exhibit Hall 3, America's Center

[H33.61] Dynamics of surface chemical reactions induced by low-energy electrons:oxydation of hydrogen passivated Si by H_2O

Dimitri Klyachko, Paul Rowntree, Leon Sanche (University of Sherbrooke, Quebec, Canada)

From dklyachk@courrier.usherb.ca Thu Feb 15 17:03:32 1996 Received: from courrier.usherb.ca by aps.org (8.6.12/1.35) id VAA15070; Thu, 15 Feb 1996 21:52:36 GMT Received: from [132.210.159.58] by courrier.usherb.ca (AIX 3.2/UCB 5.64/4.03) id AA24199; Thu, 15 Feb 1996 16:56:09 -0500 Date: Thu, 15 Feb 1996 16:56:09 -0500 Message-Id: <9602152156.AA24199@courrier.usherb.ca> X-Sender: dklyachk@courrier.usherb.ca Mime-Version: 1.0 Content-Type: text/plain; charset="us-ascii" To: abs-submit@aps.org From: dklyachk@courrier.usherb.ca (Dimitri Klyachko) X-Mailer:

\documentstyle[11pt,apsab]article \nofiles

\MeetingIDMar96

\SubmittingMemberSurnameSanche \SubmittingMemberGivenNameLeon \SubmittingMemberEmailIsanche@courrier.usherb.ca \SubmittingMemberAffilDepartment of Nuclear Medicine, University of Sherbrooke, Quebec, Canada

\PresentationTypeposter

\SpecialInstructions

\SortCategory37d \DPPType

\lognumber115 \received15 Feb 1996 \begindocument

\TitleDynamics of surface chemical reactions induced by low-energy electrons:oxydation of hydrogen passivated Si by H_2O

\AuthorSurnameKlyachko \AuthorGivenNameDimitri \AuthorSurnameRowntree \AuthorGivenNamePaul \AuthorSurnameSanche \AuthorGivenNameLeon

The dynamics of surface chemical reactions induced by low energy electrons have been studied using a model system of H_2O adsorbed on a hydrogenated surface of Si. The onset of the reaction has been observed at electron energy E_p=5.2 ±0.2 eV and associated wit

Dissociative Electron Attachment of electrons to H_2O molecules. The cross-section of the surface oxidation exhibits a strong maximum at E_p 11 eV, in contrast with the gradual increase of the cross-section for water radiolysis with the increase of the electron energy reported in bulk ice. This discrepancy can be explained by a selective quenching of the excited and positively charged states of adsorbed molecules due to the resonance charge exchange between adsorbate and substrate. Partcularly, we show that excited negative ions of H_2O can be formed at the surface by coupling of the substrate electrons to neutral excited states of adsorbed H_2O molecules. A simple model has been proposed which relates the kinetics of the surface reaction induced by electrons to the rates of the radical generation in the adsorbed film and their reaction with a substrate.

- **Part H of program listing**

10/066,329 (B)

PHYS. MED. BIOL., 1969, VOL. 14, NO. 2, 305–314

Uniformity of High-Energy Electron-Beam Calibrations

MARGARETE EHRLICH, PH.D.
and
P. J. LAMPERTI, B.S.
National Bureau of Standards, Washington, D.C. 20234

Received 24 September 1968

ABSTRACT. A survey is made of the first year of operation of a new service offered by the National Bureau of Standards (NBS). Dosemeter units, consisting of polystyrene blocks holding stoppered quartz spectrophotometer cells filled with Fricke solution, are being shipped periodically to groups requesting assistance with absorbed-dose measurements in high-energy electron beams. As a check on their stability, all dosemeters are pre-exposed to ^{60}Co γ-rays. The participants irradiate a portion of the dosemeters with electrons, using energies between about 5 and 50 Mev, and doses between 4000 and 8000 rads in water. The exposed dosemeters are returned to NBS for evaluation. During the first year of operation, slightly more than one-half of the doses reported by the participants were within $\pm 5\%$ of the NBS dose interpretation, but some differed by as much as 30% or more. Little correlation was found between a participant's method of beam calibration and agreement with NBS dose interpretation.

1. Introduction

Since July 1967 the National Bureau of Standards (NBS) has been mailing Fricke dosemeter units quarterly to groups in the United States requesting assistance with absorbed-dose measurements in high-energy electron beams (Lanzl 1967; Department of Commerce 1967). This service is thought of as a stop-gap procedure, to be carried out while the NBS standard absorbed-dose calorimetry programme is under development.

In this paper, the information which NBS collected on electron-therapy equipment and procedures is surveyed briefly; material is presented on NBS's experience in the preparation, shipping and evaluation of large numbers of Fricke dosemeters; and finally, representative data and observations are given on the results obtained during the first year of the service regarding the uniformity of high-energy electron-beam calibrations for radiation therapy.

2. Survey of equipment and procedures employed by participants in NBS studies

Table 1 shows a summary of the types of electron machines used by the participants in the NBS studies, and the methods of beam broadening, monitoring and calibration. For coverage of the required treatment area, the initially narrow, monoenergetic electron beams from betatrons or linear accelerators, operating at energies between 5 and 33 Mev, usually are broadened by means of thin scattering foils of low atomic number. One institution employs a narrow, monoenergetic beam of electrons and scans the treatment

Table 1. Summary of survey results[1]

Item	No. of participants using the item
1. Type of Accelerator	
betatron	12
linear accelerator	4
2. Field Coverage by	
scanning	1
beam broadening through scattering	15
3. Range of Electron Energies (T)[2]	
$5 \leqslant T < 10$	6
$10 \leqslant T < 15$	7
$15 \leqslant T < 20$	11
$20 \leqslant T < 25$	6
$25 \leqslant T < 30$	3
$30 \leqslant T \leqslant 35$	3
4. Scatterer (or Scanner)-to-Phantom Distance (d)	
$d < 50$ cm	4
$50 \text{ cm} \leqslant d < 100$ cm	7
$d = 100$ cm	3
$100 \text{ cm} < d < 150$ cm	1
5. Cone Material	
aluminium	3
brass	1
steel	4
lead	3
aluminium-brass-combination	1
6. Collimating Diaphragm Material	
graphite	1
aluminium	3
brass	1
steel	1
lead	2
aluminium-steel-lead-steel combination	1
7. Accelerator-Tube Window Material	
beryllium	7
aluminium	1
plastic	1
glass	1
ceramic	3
nickel	1
8. Scattering, Foil Material[3] and Thickness	
aluminium (0·03)†	4; $5 \leqslant T \leqslant 20$ Mev
nickel (0·008)	1; $T = 6$ Mev
stainless steel (0·005)	1; $T = 8$ Mev
copper (0·010–0·014)	2; $15 \leqslant T \leqslant 35$ Mev
lead (0·010–0·024)	4; $15 \leqslant T \leqslant 22$ Mev
aluminium (0·03)+lead (0·01)	6; $8 \leqslant T \leqslant 25$ Mev
copper (0·01)+lead (0·013)	1; $T = 33$ Mev
9. Monitor	
transmission ion chamber	12
cavity chamber	3
10. Beam Calibration[4]	
(a) absorbed-dose calorimeter	
at participant's institution	2
elsewhere (indirect calibration)	3
(b) Fricke dosemeter (G=15·5 or 15·6/100 ev)	
at participant's institution	2
elsewhere (indirect calibration)	2
(c) Faraday cage; absorbed dose computed from flux density	1
(d) various ionization chambers[5]	
calibrated against (a) or (b)	6
without correction	4
(e) thermoluminescence dosemeters[6]	2

† The numbers in the parentheses are thicknesses in inches, most of them as supplied by the participants.

[1] Not all participants responded, and not all of those responding answered all questions.
[2] All but a few participants used more than one energy.
[3] For some, the accelerator tube window acted as the scatterer.
[4] Some participants used more than one method.
[5] Siemens, Victoreen, and Baldwin–Farmer.
[6] Calibrated with ^{60}Co γ-rays in terms of absorbed dose in polystyrene.

area. There is considerable variation in the physical facilities (type of accelerator; materials used for beam window, collimator, and cone; scatterer-to phantom-distance). To calibrate their beams, several groups use absorbed-dose calorimetry (either directly or indirectly via measurements with another instrument, for example, an ionization chamber calibrated against an absorbed-dose calorimeter), or Fricke dosimetry. Others use ionization chambers or LiF thermoluminescence dosemeters calibrated with ^{60}Co γ-rays in terms of absorbed dose in a phantom, and apply correction factors relating the response of their dosemeter to ^{60}Co γ-rays and to high-energy electrons. Still others employ ionization chambers calibrated with ^{60}Co γ-rays in terms of exposure, placing them in the phantom used for electron irradiation, and—ignoring conceptual and other difficulties—taking their readings (in R) in the electron beam as the absorbed dose in the medium. Many groups employ more than one method.

3. The NBS Fricke Dosemeter

3.1. *Preparation*

Fricke solution, prepared according to the guidelines of the American Society for Testing Materials (ASTM Standards 1965), is used in silica cells which, in turn, are cradled in polystyrene blocks. The units are shown in fig. 1. The glass-stoppered silica spectrophotometer cells were chosen because of their resistance to radiation damage, and because the use of plastic containers would

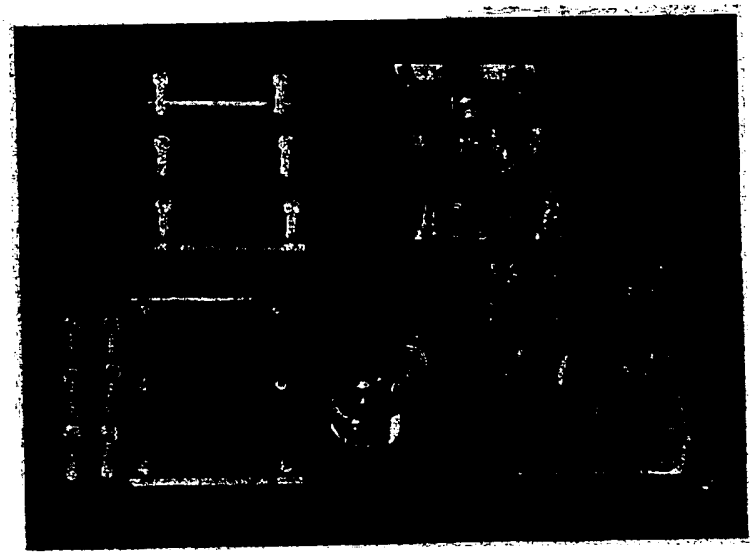

Fig. 1. Fricke dosemeter units. The spectrophotometer cell fits snugly into the polystyrene block; in the finished assembly, a styrofoam plug presses against the stopper and keeps it in place.

result in organic contamination of the solution. Under the present arrangement, handling time and sources of contamination are further reduced by keeping the Fricke solution in the stoppered cell throughout the entire process of testing, irradiation, and evaluation.

The polystyrene block is machined to fit into a recess in the polystyrene phantom recommended by the Sub-committee on Radiation Dosimetry (SCRAD) of the American Association of Physicists in Medicine (1966). The centre of the unit is at 1 cm below the surface, which is the depth recommended by SCRAD for use at the lowest electron energy employed for therapy, i.e. 5 Mev.

Prior to their first use, all cells are cleaned ultrasonically in a 0·8 N sulphuric-acid bath. Distilled and de-ionized sterile water from a commercial supplier is employed for the preparation of the Fricke solution and all cleansing procedures. A comparison of the performance of dosemeters prepared with this and with triply distilled water showed no difference in the stability and reproducibility of their densities (Pinkerton 1967). It was determined previously (Pinkerton, private communication from Memorial Hospital, New York) that, for electrons of 6 Mev and above, and for Fricke solution irradiated in a polystyrene phantom, the densities obtained with polystyrene irradiation cells agree to within the experimental reproducibility (better than 1%) with the densities obtained with quartz irradiation cells (1 mm wall thickness) for the same pathlength of solution, and the same average absorbed dose.

The cells are rinsed several times with the sterile water and the Fricke solution before the final filling is made. Because of the narrow cell necks which help

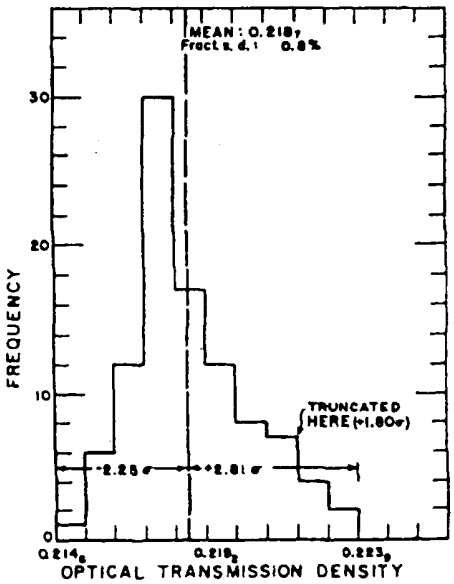

prevent spilling during shipment, but also make cleaning more difficult, the cells are emptied by aspiration and by shaking. Wash water and solution are transferred to the cells from wash bottles equipped with finely drawn-out glass spouts and pressure balloons. Glass tubing is used in all parts of the system that come in contact with these liquids.

3.2. *Test exposures*

After an initial sampling of the optical transmission density (hereafter called density) of the unexposed dosemeters, all dosemeters are exposed identically to ^{60}Co γ-rays to a density of between 0·20 and 0·25, corresponding to a dose of between 5000 and 6000 rads in water. An example of the resulting statistical distribution of the densities is shown in fig. 2. Typically, the distribution is somewhat skewed toward the higher densities. Its fractional standard deviation is slightly below 1%. In an attempt to eliminate possible unstable dosemeter cells whose densities were considerably higher than average, the

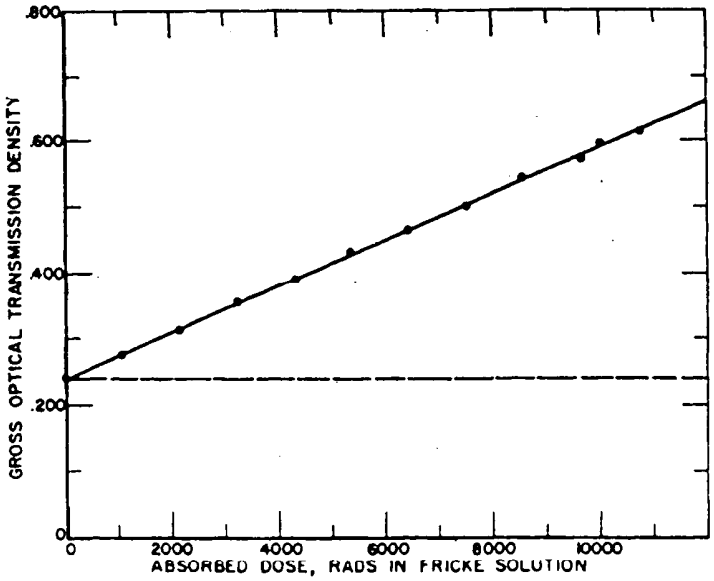

Fig. 3. Result of a test of the additivity of the response to ^{60}Co γ-rays and to high-energy electrons. The absorbed dose values plotted as abscissae are those determined by the Therapy Department of Michael Reese Hospital, Chicago, for their 33 Mev electron irradiations. The density values plotted as ordinates were obtained at NBS. The solid line through the points was obtained by a least-squares fit of the data. The dashed line represents the density level due to the initial ^{60}Co γ-ray exposures.

distribution was truncated arbitrarily, and all further work was done with the pre-exposed dosemeters whose densities were within the truncated distribution.†

A question may arise regarding the justification for using dosemeters pre-exposed to ^{60}Co γ-rays for subsequent work with high-energy electrons, particularly since the G-value of the Fricke solution may be different for the two types of radiation. Fig. 3 shows the result of a test of the additivity of the response to ^{60}Co γ-rays and to high-energy electrons for one group of Fricke dosemeters. All samples were first irradiated identically with ^{60}Co γ-rays to produce a density of about 0·24; subsequently, they were given a series of 33 Mev electron doses between 1000 and 11 000 rads in water. The G-value computed from the slope of the density-versus-electron-dose curve agreed within 1·3% with the G-value used initially to compute the absorbed dose.

3.3. *Spectrophotometry*

All densities were determined with a commercial spectrophotometer provided with a hydrogen lamp, a temperature stabilizer, and a digital read-out. The readings were carried out at 25°C, at a wavelength of 304 nm. The spectrophotometer was calibrated over the range of densities of interest with ferric-ion solutions of known molarity, made with pure iron dissolved in 0·4 M sulphuric acid, oxidized with hydrogen peroxide, and then heated to drive off excess hydrogen peroxide. The molar extinction coefficient for a given ferric-ion concentration, determined for successive calibrations of this type, is estimated to be known to within 0·1%. However, with the particular spectrophotometer used, its value depends on ferric-ion concentration, and thus on density. The change over the density range of interest (a range of about 0·22 to 0·63) is approximately 0·9% (from about 2179/mole cm to about 2160/mole cm).

4. The NBS uniformity studies

4.1. *Electron irradiation by participants*

The participants are asked to expose all but two of the furnished dosemeters to between 5000 and 8000 rads in water, at electron energies between 5 and 50 Mev, employing the exposure geometry (field size, type of phantom, position of dosemeter in phantom) recommended by SCRAD. After irradiation, the dosemeters are returned to NBS for spectrophotometric evaluation of the ferric-ion concentration in terms of the absorbed dose in the dosemeter solution.

4.2. *Evaluation of the participants' performance*

After return of the mailed dosemeter units, all dosemeters are read again, and the net density of the electron-exposed dosemeters is determined as the difference between their measured densities and the mean density of the control-dosemeter cells. An experiment was performed on one batch of Fricke solution in order to determine whether density growth with time under varying

† For the sample distribution shown in fig. 2 it later turned out that, over a period

storage conditions is a function of density level. No significant trend was observed between shipped samples and samples remaining at NBS. During the period of about four weeks between the first and second spectrophotometer readings, the average density of the control dosemeters increases by about 0·003 to 0·004. Typically, there is little difference between the standard deviations for the shipped controls and those remaining at NBS, but the distribution for the shipped controls usually is more symmetrical.

The NBS Fricke-dosimetry service is intended as an aid to other laboratories for achieving uniformity in the calibration of high-energy electron beams. A reference to absorbed dose is, therefore, not required in the NBS evaluation of the test results. However, it was felt that such a reference would be helpful. It was decided to provide an interpretation of the results in terms of absorbed dose, with the understanding that the NBS dose values will not be based on an absolute calibration procedure, but will be obtained with the aid of certain assumptions about the G-value (see below). The absorbed dose in the Fricke dosemeters was determined as

$$D_{\text{Fricke}} = (0{\cdot}942_6 \times 10^6 \times \text{net density})/(\epsilon_{Fe}^{+++} - \epsilon_{Fe}^{++})G,$$

where the constant is the product of Avogadro's number and the conversion factor from ev to rads, divided by the specific gravity of the solution; ϵ_{Fe}^{+++} is the molar extinction coefficient for ferric ions, determined experimentally for the particular spectrophotometer and the particular conditions of its use (see section 3.3); and ϵ_{Fe}^{++} is the molar extinction coefficient for ferrous ions, which was set equal to unity. The G-value was assumed to be independent of temperature over the range encountered during irradiation of the dosemeters under laboratory conditions, and to be equal to 15·5/100 ev over the electron-energy range of interest.† Also, within the limits of uncertainty of the NBS Fricke-dosimetry service, it was assumed that the dose in the Fricke-dosemeter solution could be set equal to that in water. The absorbed dose per unit fluence for the Fricke solution is only a few tenths of 1% higher than that for water (Pettersson and Hettinger 1967).

In order to test our ability to interpret the participants' irradiations, we carried out a test involving exposure at NBS of Fricke dosemeters to two levels of ^{60}Co γ-rays, mailing them to a number of participants who then returned them for evaluation. The rms value of the difference between the dose computed from exposure and that determined from readings on an individual Fricke dosemeter was about 1·5%. The corresponding 95% confidence interval for individual dosemeter readings was about 3%.

4.3. *Typical performance*

The typical overall performance of the participants as a group in a single mailing is reflected by fig. 4, in which the dose values reported by each participant

† Pettersson and Hettinger (1967) use a temperature coefficient of +0·15% per °c. For data on the trend of G with LET, see, f.i., ICRU Report 10 b (1964).

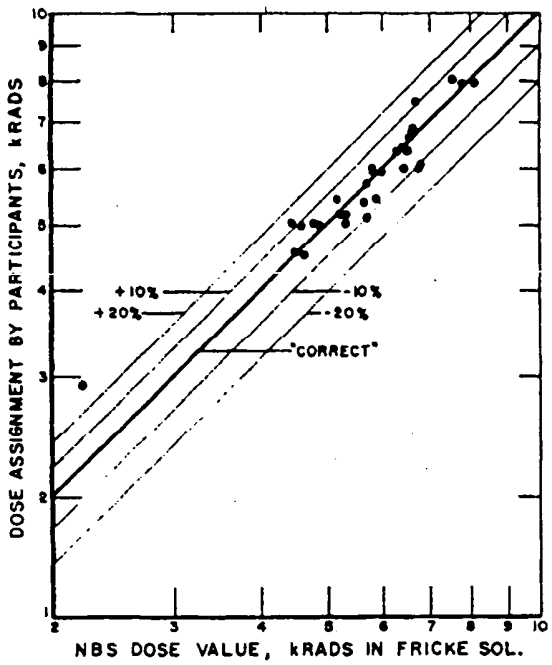

Fig. 4. Overall performance of the participants as a group in a single mailing.

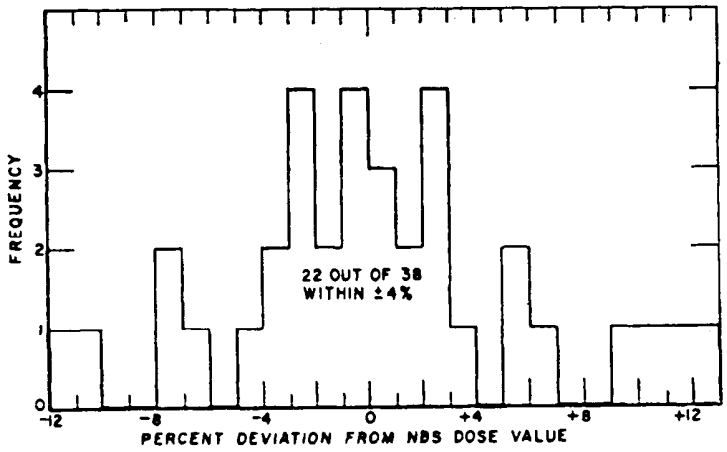

Fig. 5. Statistical evaluation of the dose data shown in fig. 4. Not plotted are three reported dose values that deviated from the NBS dose interpretation

are plotted on a log–log plot against the values determined at NBS. Along the heavier 45-degree line marked " correct ", the values assigned by the participants agree with the NBS dose interpretation. The other lines are the boundaries of regions in which the deviation from the " correct " values is smaller than the indicated boundary value. Fig. 5 shows the results of a statistical evaluation of the dose data shown in fig. 4. The distribution is slightly skew, indicating that there is a tendency for the dose reported by the participants to be somewhat higher than that determined at NBS. In 22 out of 38 cases, the participants' dose assignment was within ±4% of the NBS dose evaluation.

So far, NBS has carried out four tests. In some instances, the agreement between the doses reported by the participants and the NBS dose interpretation improved with subsequent tests, but not in all. Little or no correlation could be found between the extent of agreement with NBS and the method used for calibrating the electron beam. Nagl and Sanielevici (1967) had similar experiences in their international comparisons.

4.4. *Future work*

In the hope that the NBS Fricke-dosimetry service is contributing to an improvement in the uniformity of therapy dosimetry in the United States, it is planned to continue it, if there is demand, at least up to the time that NBS will be in a position to offer an absorbed-dose calorimetry service.

We wish to thank Dr. Jaques Ovadia and his staff of Michael Reese Hospital, Chicago, for administering the electron irradiations required for the study of additivity of the response of the Fricke-dosemeters to electrons and ^{60}Co γ-ray photons. We also wish to thank Mr. Arthur Pinkerton of the Sloan-Kettering Institute, New York, and Dr. Peter Almond of M.D. Anderson Hospital, Houston, for assisting in the planning of the service, and Mr. Erle Deardorff of NBS for carrying out the spectrophotometer readings.

The work was supported in part by the U.S. Public Health Service, National Center for Radiological Health.

Résumé

L'uniformité des calibrations avec des faisceaux d'électrons de haute énergie

On rend compte de la première année du fonctionnement d'un service nouveau existant au National Bureau of Standards (NBS). Des dispositifs dosimétriques, composés des blocs polystyrène portant des cuvettes spectrophotométriques en quartz avec bouchon, remplies de la solution Fricke, sont envoyés périodiquement aux groupes qui voudraient être aidés dans les mesures de la dose absorbée en cas de faisceaux d'électrons de haute énergie. Pour contrôler leur stabilité tous les dosimètres sont exposés préalablement aux rayons gamma du ^{60}Co. Les participants irradient une partie de dosimètres avec des électrons, en employant des énergies entre 5 et 50 Mev environ, et des doses entre 4000 et 8000 rads en l'eau. Les dosimètres exposés sont retournés au NBS pour être évalués. Pendant la première année du fonctionnement, un peu plus que la moitié de doses communiquées par les participants ne différait plus que de ±5% de la dose d'interprétation de NBS, mais pour quelques doses la différence s'élevait à 30% ou davantage. On a trouvé peu de corrélation entre la méthode employée par le participant pour la calibration du faisceau et l'accord avec la dose d'interprétation de NBS.

Zusammenfassung

Gleichförmigkeit der Kalibrierung mittels energiereicher Elektronenstrahlen

Es wird eine Übersicht ausgeführt für das erste Arbeitsjahr der vom National Bureau of Standards (NBS) angebotenen Dienstleistungen. Dosimetergeräte bestehend aus Polystyrolblöcken mit einer verschlossenen, mit Frickelösung gefüllten Spektrophotometer-Quarts-Küvette, werden periodisch an Gruppen ausgesandt, welche um Hilfe in Messungen der absorbierten Dosis mit energiereichen Elektronenstrahlen bitten. Als Stabilitätskontrolle were alle Dosimeter zuerst ^{60}Co-Gammastrahlen ausgesetzt. Die Teilnehmer bestrahlen einen Teil dieser Dosimeter mit Elektronen, wobei Energien von ungefähr 5 bis 50 Mev, und Dosen zwischen 4000 und 8000 rad im Wasser angewandt werden. Die bestrahlten Dosimeter werden an das NBS zur Bewertung zurückgesandt. Im Laufe des ersten Arbeitsjahres, etwas mehr als die Hälfte der von den Teilnehmern gemeldeten Dosen waren innerhalb der Grenzen von ±5% von der NBS-Dosis-Deutung verschieden, doch betrug der Unterschied in manchen Fällen 30% oder mehr. Es wurde eine unbedeutende Korrelation gefunden zwischen dem vom Teilnehmer angewandten Strahlen-Kalibrierungsverfahren und der Übereinstimmung mit der NBS-Dosis-Deutung.

Резюме

Единообразие калибровок электронных лучей большой энергии

Представлен отчет первого года существования новой службы, предлагаемой Национальным бюро стандартов (НБС) США. Дозиметрические установки, состоящие из полистироловых блоков с вакупоренными кварцевыми спектрофотометрическими кюветами, наполненными раствором Фрикке, отправляются периодически к группам, нуждающимся в содействии при замерах поглощенной дозы в случае электронных лучей большой энергии. Для проверки их стабильности все дозиметры подвергаются предварительно облучению гамма-лучами из ^{60}Co. Участники облучают часть дозиметров электронами, применяя энергии от около 5 до 50 Мэв и дозы между 4000 и 8000 рад в воде. Облученные дозиметры возвращаются в НБС для оценки. В течение первого года работы немногим более половины доз, указанных участниками, находилось в пределах ±5% от интерпретации дозы НБС, но некоторые дозы разнились на 30% или больше. Слабая корреляция была найдена между методом, употребленным участником для калибровки лучей, и согласием с интерпретацией дозы НБС.

References

ASTM Standards, 1965, Designation D 1671–63; *Book of ASTM Standards, Part* 27 (Philadelphia: American Society for Testing and Materials).

Department of Commerce, 1967, *Federal Register*, **32**, No. 251, Part II.

International Commission on Radiological Units and Measurements (ICRU), 1964, *Report* 10b, 1962, *National Bureau of Standards Handbook* 85.

Lanzl, L., 1967, *Radiology*, **88**, 595.

Nagl, J., and Sanielevici, A., 1967, *Strahlentherapie*, **133**, 561.

Pettersson, C., and Hettinger, G., 1967, *Acta Radiol.*, **6**, 160.

Sub-Committee on Radiation Dosimetry (SCRAD) of The American Association of Physicists in Medicine, 1966, *Phys. Med. Biol.*, **11**, 505.

10/066,329 (1)

Nanotechnology **13** (February 2002) 38-42

High-pressure nanolithography using low-energy electrons from a scanning tunnelling microscope

Brandon L Weeks[1], Antje Vollmer[1], Mark E Welland[2] and Trevor Rayment[1,3]

[1] Department of Chemistry, Lensfield Road, Cambridge University, Cambridge CB2 1EW, UK

[2] Department of Engineering, Trumpington Street, Cambridge University, Cambridge CB2 1PZ, UK

[3] Author to whom any correspondence should be addressed.
E-mail: tr22@cam.ac.uk

Received 24 August 2001, in final form 2 November 2001
Published 12 December 2001

Abstract. We present a reproducible method of producing nanometre-size holes on a graphite surface with a high-pressure scanning tunnelling microscope. Holes were only observed at pressures above 5 bar with voltage pulses in the field-emission range (±4-10 V). The depth of the hole varied with the pressure while the observed diameter was independent of the applied pressure. The results obtained in the presence of elevated pressures of dry nitrogen, oxygen, and argon are presented.

URL: stacks.iop.org/0957-4484/13/38
DOI: 10.1088/0957-4484/13/1/308
PII: S0957-4484(02)28284-7

 - choose format -

◂ Previous article | Next article ▸ | This volume ▴ | Table of contents ▲

CONTENT FINDER Nanotechnology

Full Search Help Author: Vol/Year: Issue: Page/Article No: Find

EJs home | EJs Extra | Journal home | Search | Authors | Referees | Librarians | User Options | Help | Recommend this journal

10/066,329

(D)

[next page (Sect 5.1)] | [previous page (Sect 4.15)] | [index] | [top]

4.16 Energy deposition by low energy electrons in Ar and other gases

H. Bichsel

In the collisions of ultra-relativistic heavy ions, the trajectory ('track') of thousands of emerging particles are measured in time-projection-chambers (TPC). An important datum for this purpose is the localization of segments of the particle tracks in small volumes. The localization in the plane perpendicular to the particle velocity is given by the extent of the cloud of ionization produced by the particles, typically averaged over segments of a few centimeters of track. For particles with charge ±1, for about 80% of the segments ('pads' in current slang) the ionization cloud in gas at 1 atm has a diameter of less than 0.1 mm. For the others secondary electrons ('δ-rays') with energies exceeding 5 keV will produce ionization further from the track, and the position of such segments will be known with a larger uncertainty. In order to determine these uncertainties, the spatial distribution of the ionization by the δ-rays must be known. Also, we must know the spectrum of δ-ray energies. A fairly good approximation to this spectrum can be obtained with the Fermi-virtual-photon method, as outlined in earlier reports. This method is also known as the Weizsäcker-Williams or PAI method.[1] The spatial distribution of the energy deposited or, more appropriately, the ionization has been measured for electrons with energies up to about 5 keV in some gases, but not in Ar. A Monte Carlo program for the calculation of these distributions has been obtained from B. Grosswendt (at Physikalisch-Technische Bundesanstalt in Braunschweig), and is being investigated at present. Only preliminary results have been obtained so far, and need confirmation. Corresponding experiments would be very desirable.

[1] H. Bichsel, in Atomic and Molecular Physics Handbook, Ch. 87, G. Drake, ed., Amer. Inst. Phys. 1996.

[next page (Sect 5.1)] | [previous page (Sect 4.15)] | [index] | [top]

Previous abstract Next abstract

10/066,329

E

Session 18 - Flares I.
Oral session, Tuesday, July 01
Ballroom A, Chair: Mona Hagyard

[18.04] Stochastic Acceleration of Low Energy Electrons in Plasma with Finite Temperature

J. Pryadko (Stanford University), V. Petrosian (Stanford University)

In this paper we extend our earlier work (Pryadko and Petrosian, ApJ. 1997, vol.482) on the acceleration of low-energy electrons by plasma turbulence to include the effects of finite temperature of the plasma. We consider the resonant interaction of such electrons and the whole transverse branch of plasma waves propagating along the magnetic field. The importance of the plasma parameter \alpha = ømega_pe/Ømega_e (the ratio of electron plasma frequency to electron gyrofrequency) in the dynamics of the charged particles is emphasized. We show that our earlier published results for acceleration of low-energy electrons can be applied to the case of finite temperature if the sufficient level of turbulence is present. From comparison of the acceleration rate of the particles with the decay rate of the waves they interact with, we determine the energy density of waves, as a fraction of the magnetic energy density, required for acceleration of a substantial fraction of the background plasma electrons. The dependence of this value on the plasma and turbulence parameters is described through the numerical results. The approximate analytical expression is derived for the case of super-thermal electrons.

This work was supported by NSF grant ATM 93-11888 and NASA grants NAGW 1976 and 2FEX404.

Program listing for Tuesday

10/066,329

(F)

Holography with Low Energy Electrons: Principles and Applications

Hans-Werner Fink
Institute of Physics, University of Basel, Klingelbergstrasse 82, CH-4056 Basel, Switzerland

Abstract

The concept of holography with low energy electrons is described in view of its applications in molecular biology. The challenges and difficulties associated with Gabor type holography are outlined and the differences between coherent electron beams of high and low kinetic energy are discussed. The properties of the coherent electron point source for low energy electrons are reviewed as well as its application in the lens-less holographic microscope. Investigations of in-situ manipulation of objects with nanometer sized dimension will be discussed. Those experiments have recently been applied to DNA molecules and it has been discovered that DNA molecules are in fact electrically conducting bio-polymers.

Basic Concepts of Holography

Fifty years ago, the idea of holography as "a new microscopy principle" was presented by Gabor [1] as a means to circumvent the inherent spherical aberrations of electron lenses. Gabor proposed to employ a divergent electron beam, propagating beyond the focus of an electron microscope, to illuminate an object placed in the path of the beam and to record the result of the interaction between the electrons and the object at a distant detector. The geometry of this set-up is illustrated in Figure 1. At first, the schematic appears like a simple projection set-up giving rise to a magnified image of the object at the distant detector and exhibiting a contrast which is given by the ability of the object to absorb some of the incoming electrons. However, if the phase space density of the electrons is high, which implies that their spread in location $\Delta(x_1,x_2,x_3)$ in real space and momentum $\Delta(p_1,p_2,p_3)$ is sufficiently small, the electrons are coherent and have to be considered as a wave with a de Broglie wave length $\lambda=h/p$. In such a situation, the divergent beam beyond the point focus of the electron microscope has to be regarded as a propagating coherent spherical wave which is impinging onto the object under study. Most of the wave will pass the object without interactions and arrive at the detector to form a coherent background. This part of the wave is referred to as the reference wave. A much smaller fraction of the primary coherent wave front is elastically scattered at the object. This gives rise to a phase shift in comparison with the primary wave. Since the elastic scattered wave is coherent with the reference wave, the two wave fields are able to interfere and form a fringe pattern at the detector. The intensity distribution of this record

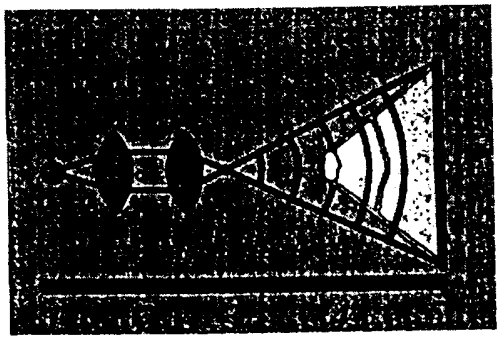

Figure 1: Schematic showing the set-up of an electron microscope to be employed for holography according to Gabor. 1: Electron Source. 2: Electron optical column. 3: The focus of the electron microscope is the de-magnified image of the primary electron source. 4: Object that scatters some of the coherent electrons. 5: Detector to record the hologram which arises from the interference between the coherent background and the part of the wave that experienced scattering by the object.

is determined by the constructive and destructive interference between reference and object wave. This justifies the term "holo" inasmuch as the "complete" information about the object wave, namely its amplitude and phase, is contained in this two-dimensional record. While the complete information about the object is available in the

[illegible]

the desired microscopy information about the object from its hologram [illegible] achieved [illegible]

fundamental optical principles of diffraction. Given an object, determined in its shape by an object function, the Huygens-Fresnel-Kirchhoff theory describes the hologram as a transformation applied to this object function. In order to derive the object function again from this interference pattern, the

inverse transformation is applied to the holographic record. Physically, this corresponds to illuminate the hologram again with the same type of radiation as during the recording process of the hologram; however in the absence of the object. The waves arising from scattering at the hologram interfere in such a way as to reveal the shape of the wave front at the object. Another way to visualize the process of the hologram reconstruction is to regard all the elementary waves that form the hologram by interference as "back-propagating waves" that converge to form a real image of the object. The major handicap of in-line holography is the twin image problem, a second image of the object that appears in the reconstruction process. This twin image is a real image, located at twice the source-object distance opposite to the hologram plane. Since this two images are situated on the same axes, there is always the out of focus twin image superimposed on the primary image. A number of proposals and some attempts have been made to eliminate this disturbing background arising from the twin image. The easiest way to at least minimize the twin-image contribution is to arrange the geometry of the set-up accordingly. This can be accomplished by positioning the object at a distance from the source that is large compared to the size of the object under study. This arrangement ensures that the twin image is largely out of focus at the position where the primary image is evaluated and thus its background contribution will nearly be constant over the area covered by the object. This provision defines the field of sensible utilization of in-line holography to small objects that cover only part of the coherent wave front.

Early attempts of electron holography [2] following Gabor's insight did not lead to any practical applications due to the lack of sufficient bright electron sources at this time. Following the invention of the Laser, it was subsequently experimentally realized that Gabor's ideas proved to be correct. Furthermore, light optical holography became a tool with great practical applications. However, as mentioned already above, Gabor's original in-line holography concept proved to be limited to the study of small particles by employing pulsed laser beams. Laser-holograms of larger objects are exclusively taken in the off-axes geometry that was introduced by Leith and Upatnieks [3]. They came up with an effective way to eliminate the twin image problem by splitting the primary beam to physically separate the path of the object wave from that of the reference wave. The invention of the biprism for electrons by Möllenstedt [4] made the off-axes geometry also accessible to holography with electrons. As one can recognize by the contribution of H. Lichte [5] in this issue, off-axes electron holography has become an impressive domain of ultra high resolution electron microscopy.

Since the early efforts by Heine and Mulvey [2] to realize in-line holography experimentally with a conventional electron microscope, significant progress has been made over the decades to improve on the brightness of electron sources, which happened to be one of the major problems in the early days of electron holography. However, in-line electron holography with conventional electron microscopes still has its challenges and problems. They are primarily associated with the high kinetic energy of the electrons, which is in the 100 keV regime. They account for two major problems, the weak phase contrast and the radiation damage, that happens to be particular disturbing in studies of organic or biological objects. Despite all those complications, progress has been made by Tonomura et al. [6] in successfully employing high energy electron beams to perform Gabor type in-line holography.

An entirely different approach to electron holography has become possible after the invention of an electron point source which by itself provides a coherent electron ensemble without the need for lenses to optically de-magnify a more extended source.

The Electron Point Source

images, presented in Figure 2, one can assess that the electric field at the tip apex is only enhanced above an atomically small region, defined by the small protrusion created by three or ultimately just one atom. By reversing the polarity at this structure, field emission occurs by tunnelling of electrons from the metal into the vacuum. The energy spread of the emitted electrons is determined by the shape of the tunneling-barrier foldet with the density of states of the electrons near the Fermi energy.

This accounts for a fairly monochromatic electron beam with an energy distribution width around 200 meV. Inasmuch as the emission area is of atomic size and comparable to the de Broglie wave length of the electrons, we expect the emitted free electron ensemble to be highly coherent. This electron point source can consequently be used to carry out interference experiments in a conceptually simple set-up just as easy as with a Laser in light optics. If, for example, the electron point source is placed in front of two holes in a thin gold foil and a potential of 75 Volts is applied to emit electrons that impinge onto the foil structure, the well known Young double slit interference fringes can be detected some centimetres away from the foil, as displayed in Figure 2. In principle, coherent sources are simple to achieve. Even before the invention of the Laser a coherent light source could be made by just filtering light from an extended source and selecting a micrometer diameter aperture. However, the brightness of such a coherent light source is extremely low and it is therefore of little use compared to a Laser. Fortunately, our electron point source does not just directly deliver coherent electrons without the need for apertures and lenses, but it does so at a maximal rate which is of the order of 10^{15} electrons per second which relates to currents in the mA regime [9].

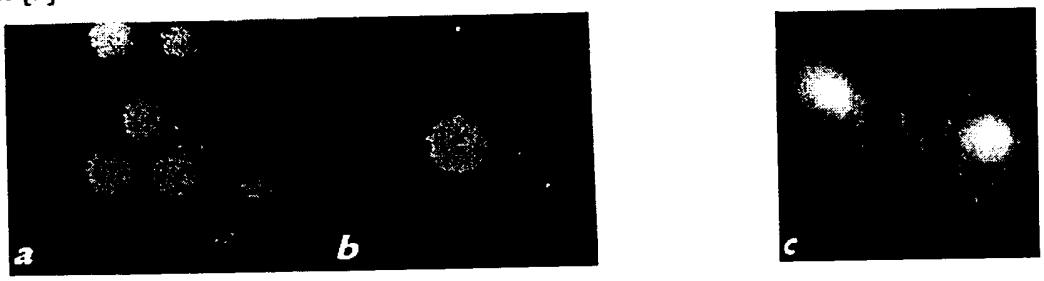

Figure 2: Helium field ion images taken from the top two layers of the ultimate smallest pyramid made up of tungsten atoms. A cluster of three atoms (a) support the individual atom that forms the top of the pyramid (b). The interference fringes observed behind two holes in a thin gold foil (c) show that the electrons with 75 eV kinetic energy originating from the point source are actually coherent.

Holography with Low Energy Electrons

With a bright and coherent electron source there is no need anymore to employ an electron optical column to perform holography [10]. After all, the main purpose of electron lenses in the classical electron holography set-up is to obtain a highly de-magnified image of the more extended primary source of the electron microscope. Even the electron guns of modern field emission electron microscopes employ sources that are at least three orders of magnitude larger than an atomic point source. We shall see that doing away with lenses does not just simplify the design and eliminate aberrations that are intrinsic to electron lenses, but it defines an entirely different interaction scenario between the electrons and the object due to the possibility to operate at low kinetic electron energies.

The schematic, following Gabor's ideas, as illustrated in Figure 1, reduces now essentially to the one shown in Figure 3 which contains only three basic elements. Element one: the source that prepares the coherent spherical electron wave front. Element two: the object that is to be examined. Element three: a detector that records the result of the interference between the scattered wave and the coherent background. Since the key to this microscope is the electron point source we used the term 'Low Energy Electron Point Source (LEEPS) - microscope' for this tool. The in-line hologram of a

energy of the electrons which amounts to 80 eV in this particular case. This image of a carbon sample does already clearly indicate the distinction of the LEEPS microscopy from conventional electron microscopy. High energy electron microscopy experiments frequently use carbon as a support to image heavier metal atoms like gold for example. Carbon with its low z-number is one of

the best, because almost transparent, supports for electrons in the 100 keV range. In contrast to this, the low energy of the electrons and the associated scattering mechanism produce high contrast even for atoms with a low z-number. As of today, no practical analogue to the transparent carbon films for high energy electron microscopy is known for the low energy regime, other than vacuum. This puts certain demands on the sample preparation inasmuch as the objects under study have to be surrounded by enough empty space. It turns out that this is not a severe constraint. Compact objects like clusters can be placed onto fibres that span holes, as for example in carbon films, and chain-like objects like polymers can be spanned over holes in a support film. In the latter case one might even argue that the molecule is in a more 'natural' state compared to being adsorbed onto a surface of a support film. In any event, the low energy of the electrons in the LEEPS-microscope connected with the high contrast that they provide, appears to be one of the major benefits of this tool in view of the examination of molecular species that are usually made up of light atoms. A second and equally important aspect associated with the low energy is the fact that scattering at the object is mainly elastic and does not lead to noticeable radiation damage. On the other hand, the low energy narrows the application range of LEEPS microscopy to small objects due to the low penetration length. Ultra low energies of only 7 eV at which the penetration of the electrons increases again have been realized in the LEEPS microscope by Morin [11]. However, even if it would be routinely possible to operate at just a few eV kinetic electron energy, one would have to sacrifice some of the resolution potential of this tool due to the increased electron wave length. At present the experimental lateral resolution, evaluated from the reconstructed images, is in the nanometer regime. In our present design the major experimental limitation is associated with the ability to detect high order interference fringes which is due to our present 8 bit detector dynamics. The use of modern CCD detectors should help to improve the experimental resolution limit. After all, the LEEPS microscope utilizes electrons with sub-Angstrom wave length and it does not suffer from lens aberrations. Apart from the contrast and the spatial resolution, another important aspect to characterize a microscope is its time resolution. Due to the parallel detection of the LEEPS technique and its bright electron source, an entire image containing some 10^8 electrons can be acquired in a time of only some 10 µs. This is important to carry out dynamical studies.

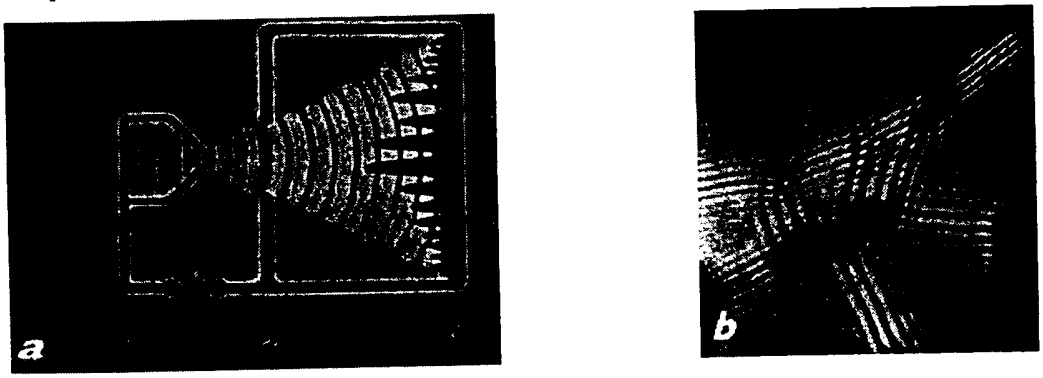

Figure 3: (a) Schematic of the Low Energy Electron Point Source (LEEPS) - microscope. 1: Electron point source. 2: Object supported on a partly transparent sample holder. 2: Detector to observe the in-line hologram. (b) A hologram of a carbon fibre network, taken with electrons of 80 eV energy, is shown.

Manipulation of Nanometer-sized Objects

their environment or within the object itself, like diffusion processes or conformational changes in clusters for example. Those observations are usually done in an ordinary thermal environment. Another challenge is to actually carry out an experiment on an object while observing it and its environment in-situ. With optical microscopes this is possible, for example by using Laser traps. Part of a biological cell can be modified or moved around while observing the entire cell at the same time.

The resolution is of course limited to that of red light which is used to not introduce radiation damage to the object. With the local probe methods, invented by G. Binnig and H. Rohrer [12], one can even manipulate samples on an atomic scale; D. Eigler [13] has shown us some time ago how to place atoms at will with an incredible accuracy. However, the sequential imaging mechanism inherent to all local probe methods allows to do only one thing at a time; that is to apply local forces at one time and to evaluate the changes on its environment at a later time. The possibilities of the LEEPS technology are at present somewhere in between that of the optical microscopy with its parallel detection and that of the scanning probe methods with its atomic resolution. With the LEEPS technology it is possible to introduce forces (mechanical or electrical) on a nanometer scale and observe the entire environment on a selected area, corresponding to a wide range of magnifications, at the same time. This includes experiments like bending or stretching objects in-situ to observe their mechanical responds while a force is acting. It also includes the application of electrical forces. An electrical potential can be applied to a certain part of a molecular structure and its response, that is generally distributed over a large area of the species, can be observed on a nanometer spatial- and 10 μs time-resolution scale.

A LEEPS microscope, in which an additional manipulation-tip has been incorporated between the sample plane and the detector, as illustrated in Figure 4, has been employed for this type of experiments. While observing the image, the manipulation-tip can be moved in a highly controlled fashion into the sample plane to contact a selected site. An example of such an experiment is also shown in Figure 4, in which the apex of a tungsten tip has been brought into contact with a carbon nanotube. The nanotube follows the motion of the tip in three dimensions while experiencing elastic deformations. The manipulation-tip can also be raised to a certain electrical potential. As a consequence, an electrical current flows through just this one selected nanotube and it can be monitored. It turns out that a single nanotube can carry some several 10 μA of current before it actually breaks. The part of the nanotube that remains attached to the manipulation tip is by itself a quite interesting object inasmuch as it can be employed as a coherent source for electrons [14].

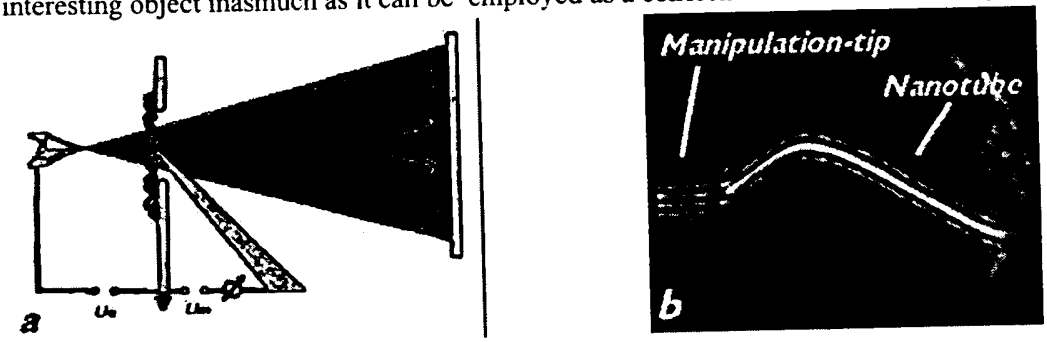

Figure 4: (a) Schematic showing the set-up to manipulate nanometer sized objects. A manipulation-tip is introduced into the LEEPS microscope to achieve mechanical contact to a selected object placed on a regular array of holes in a carbon film. An electrical potential applied to the manipulation-tip allows to probe the electrical conduction properties of the object under study. (b) A LEEPS image shows the manipulation-tip that has been guided to a nanotube that reaches over the rim of one hole of the sample holder.

Applications in Molecular Biology

The LEEPS microscope has been used to generate high contrast holograms of unstained DNA [illegible] the magnitude of the electron object wave [illegible]. Experiments to address the electrical conductivity of DNA molecules have recently been carried out by contacting individual DNA fibres by means of a manipulation-tip as described above [16]. The linear current vs. voltage curve for a 600nm long DNA fibre, shown in Figure 5, presents clear evidence for the fact the DNA molecules actually represent small conducting wires. The issue of

electrical conductivity in DNA molecules, important for example in the context of understanding repair mechanisms, was often debated but remained unsolved for a long time within the molecular biology community. Apart from the biological relevant aspects, the above mentioned results will open up the possibility to employ DNA molecules, whose chemistry happens to be extremely well understood, as tailored molecular one-dimensional conductors.

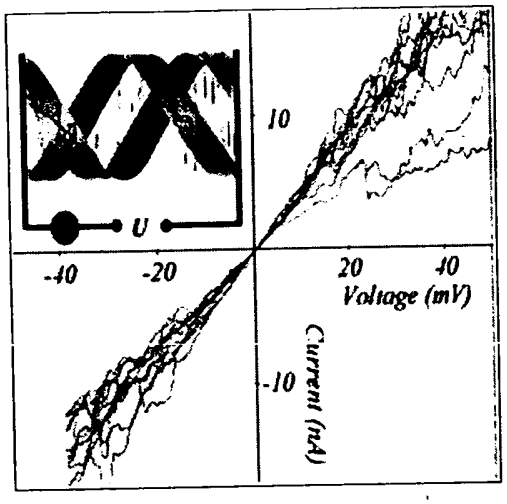

Figure 5: I-V characteristic of a 600 nm long DNA strand.

Acknowledgement:
It is a pleasure to thank my colleagues of the condensed matter physics department of the University of Basel for valuable discussions, their interest in the work presented here, and their support.

References:
[1] D. Gabor, Nature (London) 161, 777 (1948)
[2] M. E. Haine and T. Mulvey, J. Opt. Soc. Am. 42, 763 (1952)
[3] E. N. Leith, J. Upatnieks, J. Opt. Soc. Am. 52, 1123 (1962)
[4] G. Möllenstedt and H. Dücker, Z. Physik 145, 377 (1956)
[5] H. Lichte, this issue
[6] A. Tonomura, Electron Holography, Springer Series in Optical Sciences, Springer Verlag (1993)
[7] E. W. Müller, Z. Physik 131, 136 (1951)
[8] H.-W. Fink, Physica Scipta 38, 260 (1988)
[9] S. Horch , and R. Morin, J. Appl. Phys. 74 (6), 3652 (1993)
[10] H.-W. Fink, W. Stocker, and H. Schmid, Phys. Rev. Lett. 65, 1204 (1990)
[11] R. Morin, and A. Gargani, Phys. Rev. B 48 (9), 6643 (1993)
[12] G. Binnig, and H. Rohrer, Helv. Phys. Acta 55, 726 (1982)
[13] D. M. Eigler, and E. K. Schweizer, Nature 344, 524 1990); see also the individual contributions of K.-H. Rieder, W.-D. Schneider and P. Varga in this issue.
[14] H. Schmid, and H.-W, Fink, Appl. Phys. Lett. 70 (20), 2679 (1997)
[15] H.-W. Fink, H. Schmid, E Ermantraut, T. Schultz, J. Opt. Soc. Am. A (14), No. 9, 2168 (1997)
In our more recent DNA studies Quantifoil® sample supports were used provided by K. Wohlfart